Conformational and Electronic Study of *N*-acetyl-L-Isoleucine-*N*-Methylamide Using DFT and IPCM Calculations

ANA M. RODRÍGUEZ,[1] JOSEPH C. P. KOO,[2,3] DANTE E. ROJAS,[4] NÉLIDA M. PERUCHENA,[4] RICARDO D. ENRIZ[1]

[1]*Departamento de Química, Universidad Nacional de San Luis, Chacabuco 917, 5700 San Luis, Argentina*

[2]*Lash Miller Chemical Laboratories, Department of Chemistry, University of Toronto, 80 St. George Street, Toronto, Ontario, Canada M5S 3H6*

[3]*Department of Pharmaceutical Sciences, Faculty of Pharmacy, University of Toronto, 19 Russell Street, Toronto, Ontario, Canada M5S 2S2*

[4]*Laboratorio Estructura Molecular y Propiedades, Departamento de Química, FACENA Universidad Nacional del Nordeste, Av. Libertad 5460, 3400 Corrientes, Argentina*

Received 1 August 2005; accepted 29 September 2005
Published online 17 January 2006 in Wiley InterScience (www.interscience.wiley.com).
DOI 10.1002/qua.20883

ABSTRACT: A conformational and electronic study on *N*-acetyl-L-isoleucine-*N*-methylamide was carried out. All side-chain as well as backbone conformations were explored for this compound. Multidimensional conformational analysis predicts 81 structures in the case of *N*-acetyl-L-isoleucine-*N*-methylamide, 53 relaxed structures were determined at the DFT (B3LYP/6-31G(d)) level of theory. An exhaustive electronic study employing the atoms-in-molecules (AIM) method was carried out. In addition, the effects of three solvents (water, acetonitrile, and chloroform) were included in the calculations using the isodensity polarizable continuum model (IPCM) method. © 2006 Wiley Periodicals, Inc. Int J Quantum Chem 106: 1580–1595, 2006

Key words: isoleucine; conformational study; DFT; IPCM calculations

Introduction

The β-sheet formation potential (i.e., formation probability) of isoleucine (Ile) is very high [1], while the helix formation potential of Ile is average. In contrast, the global β-turn formation potential of Ile is the worst of the 20 amino acids [1]. In addition, protein conformation predicting methods are unable to predict backbone conformations of Ile residues for β-turns accurately, since they aim to predict primarily helices and sheets. Therefore, it is not surprising that peptides that include Ile residues have not been studied extensively. Although very little is known about the Ile backbone confor-

Correspondence to: R. D. Enriz; e-mail: denriz@unsl.edu.ar
Contract grant sponsor: Universidad Nacional de San Luis (UNSL), Argentina.

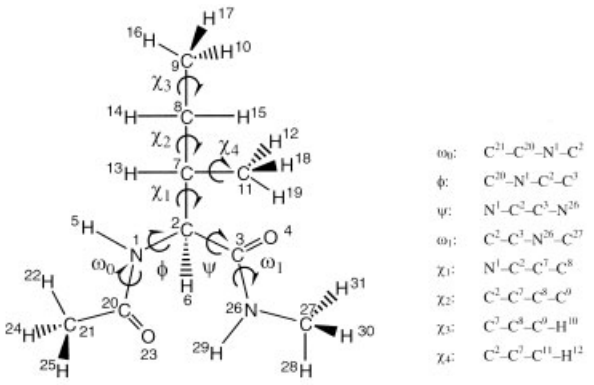

N–acetyl–L–isoleucine–*N*–methylamide (**I**)

FIGURE 1. Skeletal diagram showing the numbering of the atoms and torsional angles for *N*-acetyl-L-isoleucine-*N*-methylamide (**I**). Torsional angles are defined in terms of the atoms involved.

mations, even less is known about its side-chain conformations. In peptides, how side chains and backbones interact is a fundamental question that has not been fully answered as yet. Because of the rather large dipole moment of an amide plane, it is obvious that a charged side chain possesses a backbone conformation that influences capacity. Previous reports on *N*-acetyl-L-glutamate-*N*-methylamide [2] and Asp [3] illustrate this point very well. The same consideration takes place in the case of amino acids possessing polar side chains as for serine-NH_2 [4], *N*-acetyl-L-cysteine-*N*-methylamide [5–7], and *N*-acetyl-L-glutamine-*N*-methylamide [8]. However, it is clear that an apolar side chain may also influence the topology of an $E = E(\phi, \psi, \chi_1, \chi_2)$-type potential energy hypersurface (PEHS) as well. Previous results reported for formyl-*L*-valinamide [9–14] and more recently for *N*-acetyl-L-isoleucine-*N*-methylamide (**I**) [15, 16] (Fig. 1) support this concept.

Side-chain folding is not only interesting but also important because side-chain orientation can influence backbone folding via side-chain/backbone interactions. Of course, analysis on the phenomenon of side-chain folding requires relatively long aliphatic side chains. Ile is a higher homologue of valine; this also implies that the isoleucine side chain can reach farther out to its neighbors than can valine. For these reasons, in proteins, isoleucine may play not only a structural, but also a more extensive functional role.

From an experimental point of view, one would like to determine the number of conformers present in a given sample, their structures, their relative populations, their spectroscopic signatures, and their response to solvent and other environmental parameters. Recent studies are beginning to provide information of this type for small, flexible biomolecules in the gas phase [7, 8, 17–20].

Valine (Val) has been studied exhaustively [9–14]; however, compared with Val, Ile has received relatively little attention. As an extension of our preliminary survey of the potential energy surfaces (PES) at the RHF/3-21G [15] and RHF/6-31G(*d*) [16] levels of theory, we go beyond the previous work reporting a comprehensive study of the conformations of **I** using density functional theory (DFT) calculations and Bader analysis. Only backbone/backbone interactions were taken into account for compound **I** at the levels of theory previously reported [15, 16]. However, it is evident that to determine weak hydrogen bonding (—C—H…O—) in this amino acid residue more precisely, a higher level of calculations, including electron-correlation and Bader analysis, are needed. Also, a problem of considerable interest for the understanding of the chemistry of Ile is the determination of the most stable configurations of the molecule in solution, most importantly in water. There is, of course, a complementary but related problem: structural organization of the solvent around this compound. Our approach to understanding Ile conformational intricacies is to examine the properties of isolated Ile molecules to elucidate the role of the solvent. By first understanding the behavior of the isolated molecule in detail, it should be possible to observe the effects due to the solvent by comparing the calculations with and without solvent effects.

For all these reasons, we report the conformational PEHS of **I** from DFT calculations. An exhaustive electronic study employing the atoms-in-molecules (AIM) method [21] was also carried out. Bader established the way to characterize the intramolecular hydrogen bondings by the analysis of the electronic charge density in the bond critical points. This methodology is used to establish the presence of hydrogen bonding in the different conformations. The application of this theory serves to understand the factors that stabilize the low-energy conformations of amino acids in greater detail. It is an interesting approach which has been recently employed by our group on glutamate [2] and glutamine [8]. In addition, the effect of three solvents

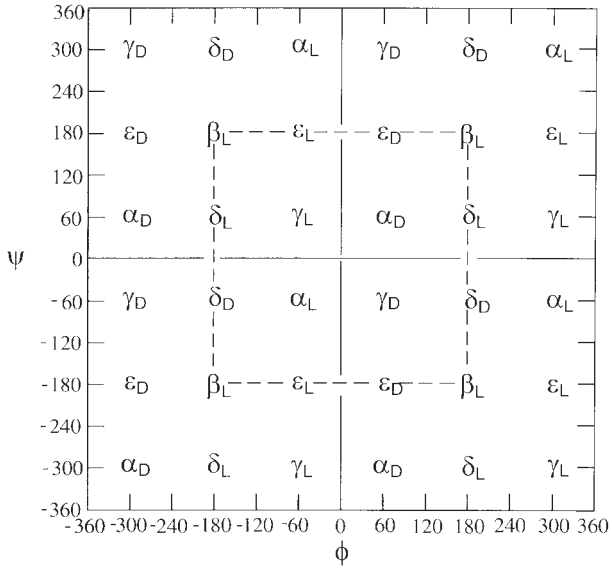

FIGURE 2. Topological representation of the Ramachandran map for an N- and C-protected amino acid PCO-NH-CHR-CO-NHQ (P and Q may be H or CH_3) showing two full cycles of rotation: $-360° \leq \phi \leq +360°$; $-360° \leq \psi \leq +360°$. The central box, denoted by broken line, represents the cut suggested by the IUPAC convention. The four quadrants denoted by solid lines are the conventional cuts. Most peptide residues exhibit nine unique conformations labeled as $\alpha_D(\alpha_{LEFT})$, ε_D, $\gamma_D(C_7^{ax})$, $\delta_L(\beta_2)$, $\beta_L(C_5)$, $\delta_D(\alpha')$, $\gamma_L(C_7^{eq})$, ε_L (polyproline II), and $\alpha_L(\alpha_{RIGHT})$.

(water, acetonitrile, and chloroform) were included in the calculations using the isodensity polarizable continuum model (IPCM) method [22].

Methods

NOMENCLATURE AND ABBREVIATIONS

IUPAC-IUB [23] rules recommend the use of $0° \rightarrow +180°$ for clockwise rotation and $0° \rightarrow -180°$ for counterclockwise rotation. For side-chain rotation, this implies the following range: $-180° \leq \chi_1 \leq 180°$, $-180° \leq \chi_2 \leq 180°$, $-180° \leq \chi_3 \leq 180°$, $-180° \leq \chi_4 \leq 180°$. On the Ramachandran map (Fig. 2), the central box denoted by a broken line ($-180° \leq \phi \leq 180°$ and $-180° \leq \psi \leq 180°$) represents the cut suggested by the IUPAC convention. The four quadrants denoted by solid lines are the traditional cuts. Most peptide residues exhibit nine unique conformations, labeled as $\alpha_D(\alpha_{left})$, ε_D, $\gamma_D(C_7^{ax})$, $\delta_L(\beta_2)$, $\beta_L(C_5)$, $\delta_D(\alpha')$, $\gamma_L(C_7^{eq})$, ε_L, and $\alpha_L(\alpha_{right})$.

However, for graphical presentation of the side chain conformational potential energy surface (PES), we use the traditional cut ($0° \leq \chi_1 \leq 360°$ and $0° \leq \chi_2 \leq 360°$), similar to that suggested previously by Ramachandran and Sasisekharan [24].

COMPUTATIONS OF MOLECULAR CONFORMERS

Molecular geometry optimizations were performed at the DFT [B3LYP/6-31G(*d*)] level of theory, using the Gaussian 98 [25] program employing standard basis set with no modifications. The importance of including electronic correlations in the conformational study has been previously reported [26]. Recently, Improta et al. [27] reported that conventional DFT methods employing periodic boundary conditions give an accurate description of both the geometry and the relative energy on these kinds of molecular systems. Correlation effects were included in the present work using DFT with the Becke3–Lee–Yang–Parr (B3LYP) [28] functional and the 6-31G(*d*) basis set. Convergence criteria were according to the limits imposed internally by Gaussian 98. With any conformational search, it is very important to examine the structures obtained to make sure that they are true minima, and not transition structures or other structures with very low or zero forces on the atoms (stationary points).

STABILIZATION ENERGIES

The stabilization energies were calculated with respect to the $\gamma_L(C_7)$ backbone conformation of N- and C-protected glycine [29, 30], using the following isodesmic (same number of the same type of bonds) reaction, where side chain R = CHMe-Et

$$\underset{\text{reference conformation } \gamma_L}{\text{MeCONH-CH}_2\text{-CONHMe}} + \text{CH}_3\text{-}\mathbf{R} \rightarrow \underset{\text{conformation X}}{\text{MeCONH-CH}\mathbf{R}\text{-CONHMe}} + \text{CH}_3\text{-}\mathbf{H}. \quad (1)$$

The stabilization energy may be calculated as follows:

$$\Delta E_{\text{stabilization}} = \{E[\text{MeCONH-CH}\mathbf{R}\text{-CONHMe}]_X + E[\text{CH}_3\text{-}\mathbf{H}]\} - \{E[\text{MeCONH-CH}_2\text{-CONHMe}]_{\gamma L} + E[\text{CH}_3\text{-}\mathbf{R}]\}. \quad (2)$$

The component's energy values are summarized in Table I.

TABLE I

Total energy values of all component molecules in the isodesmic reaction calculated at the B3LYP/6-31G(*d*) level of theory.

Molecular system	Energy (hartree)
Me—CONH—CH_2—CONH—Me (γ_L)	−456.5375160
CH_3—H	−40.5183890
CH_3CHMe—Et	−197.7711444

TOPOLOGICAL ANALYSIS OF ELECTRON DENSITY

The aim of the theory of atoms in molecules (AIM), developed by Bader et al. [21, 31] is extracting chemical insights from modern ab initio wave functions. This was applied extensively to study different chemical properties [32–39]. The topological properties of rho [ρ(r)] [21] are used for the characterization of chemical bonds in a molecular system. The AIM theory uses the electron density, a physical property of the total system, as its starting point, regardless of how it was obtained. One example of this is the partition of experimental electron densities of a molecule into atoms in terms of the gradient vector field of $\rho_{(r)}$ following the AIM theory. Since 1960 the distribution of the electronic density charge $\rho_{(r)}$, as a physical observable, has been determined experimentally by means of the diffraction of x-rays [40a]. Nevertheless, the study of molecules of medium size (20–30 atoms) with the use of conventional diffractometers and by means of a serial detection technique required periods of time as long as several weeks or even months. These difficulties meant that only qualitative results were obtained for molecules of larger size (i.e., proteins [40b]). Although during the past few years several developments have improved this situation substantially (synchrotron radiation at low temperature and new and better area detectors [41]) the most refined results of $\rho_{(r)}$ required days. Thus, these restrictive experimental conditions demand that theoretical calculations be used to make valuable contributions. A deep knowledge of the electronic structure of these conformers is essential in order to understand the mechanisms that occur during the folding of proteins.

The topological analysis and the evaluation of local properties are carried out by means of the AIMPAC program [42] using wave functions obtained at the RHF level of theory and the 6-311++G** basis set provided by the Gaussian 98 package [25].

We only present the essential theoretical information needed for the discussion of the numerical results, because the use of the topological concepts is well documented in the standard literature [21, 43].

This theory is based on the critical points (CP) of the molecular electronic charge density, $\rho(\mathbf{r})$. These are points where the electronic density gradient $[\nabla\rho(\mathbf{r})]$ vanishes and are characterized by the three eigenvalues $[\lambda_i\ (i = 1, 2, 3)]$ of the Hessian matrix of $\rho(\mathbf{r})$. The CP are labelled according to their rank as (r, s), i.e., r (number of nonzero eigenvalues) and signature s (the algebraic sum of the signs of the eigenvalues).

In molecules four types of CP are of interest: (3, −3), (3, +3), (3, +1), and (3, −1). A (3, −3) point corresponds to a maximum in $\rho(\mathbf{r})$ characterized by $\nabla^2\rho(\mathbf{r}) < 0$. It occurs generally at nuclear positions. A (3, +3) point indicates electronic charge depletion and it is characterized by $\nabla^2\rho(\mathbf{r}) > 0$. It is also known as box critical point. The (3, +1) points or ring critical points are saddle points. Finally, a (3, −1) point or bond critical point is generally found between two neighboring nuclei indicating the existence of a bond between them. In this study, the only critical points analyzed are the (3, −1) points.

Several properties that can be evaluated at the bond critical point (BCP) constitute very powerful tools to classify the interactions between two fragments [44–47]. The two negative eigenvalues of Hessian matrix (λ_1 and λ_2) measure the degree of contraction of ρ_b perpendicular to the bond toward the critical point while the positive eigenvalue (λ_3) measures the degree of contraction parallel to the bond and from the BCP toward each of the neighboring nuclei. When the negative eigenvalues dominate, the electronic charge is locally concentrated within the region of the BCP leading to an interaction typical of covalent or polarized bonds. This interaction is characterized by large ρ_b values, $\nabla^2\rho_b < 0$, $|\lambda_1|/\lambda_3 > 1$, and $G_b/\rho_b < 1$, being G_b the local kinetic energy density at the bond critical point. In contrast, if the positive eigenvalue is dominant the electronic density is locally concentrated at each atomic site. The interaction is referred to as a closed-shell interaction, and it is characteristic of highly ionic bonds, hydrogen bonds, and van der Waals interactions. It is characterized by relatively low ρ_b values, $\nabla^2\rho_b > 0$, $|\lambda_1|/\lambda_3 < 1$, and $G_b/\rho_b > 1$. Finally, the ellipticity, ε, defined as $\lambda_1/\lambda_2 - 1$, indicates the deviation of the electronic charge den-

sity from the axial symmetry providing a quantitative measure of either the π character of the bond or the delocalization electronic charge. In addition, when the value λ_2 decreases and tends to zero, it is indicative of instability of bond.

Among other derived quantities, the Laplacian $\nabla^2\rho(r)$ is the sum of the curvatures in the electron density along any orthogonal coordinate axes at the point (r). The sign of $\nabla^2\rho(r)$ indicates whether the charge density is locally depleted $[\nabla^2\rho(r) > 0]$ or locally concentrated $[\nabla^2\rho(r) < 0]$. This relationship is very useful to classify the interactions.

SOLVATION EFFECTS

The effect of three different solvents (water, acetonitrile, and chloroform) was calculated by the isodensity polarizable continuum model (IPCM) method [22]. IPCM is more advanced than the polarizable continuum model (PCM) method [48] because in IPCM the cavity of a solute is defined by the electron isodensity surface, while in PCM it is defined by the van der Waals surface. The efficiency of this method has been recognized in conformational behaviors in solution for small peptides [49]. It should be emphasized, however, that the evaluation of the solvent effect implies a comparison with the gas-phase results. Thus, both sets of results with and without the solvent are required.

Results and Discussion

CONFORMATIONAL STUDY

The overall expression of the potential energy hypersurface (PEHS) for compound **I** is a function of eight variables $E = E(\omega_0, \phi, \psi, \omega_1, \chi_1, \chi_2, \chi_3, \chi_4)$. When limiting our considerations only to *trans*-peptide bonds (i.e., $\omega_0 \approx \omega_1 \approx 180°$), the full conformational space will include six torsional angles, ϕ, ψ, χ_1, χ_2, χ_3, and χ_4, as defined in Figure 1. Thus, in principle, the conformational PEHS is a function of six variables:

$$E = E(\phi, \psi, \chi_1, \chi_2, \chi_3, \chi_4). \quad (3)$$

It should be noted, however, that in our previous exploratory study [15] using isopentane to mimic the side chain of isoleucine, we found that methyl rotations may be ignored due to the fact that the —CH_3 group has only one unique orientation. In fact, only two torsional angles in the side chain need to be varied; these are the torsional angles labeled as χ_1 and χ_2 in **I**. Thus, the PEHS of **I** can be expressed as a function of only four independent variables.

$$E = E(\phi, \psi, \chi_1, \chi_2). \quad (4)$$

Because we expect three minima (g^+, a, g^-) for each of the variables, Multidimensional Conformational analysis (MDCA) [50, 51] would lead to the existence of $3^4 = 81$ conformers. These 81 conformers would be distributed evenly, i.e., nine side-chain conformers for each of the nine backbone structures. Using MDCA-predicted 81 geometries as input, we located a total of 53 conformers on the PEHS [Eq. (3)] at the DFT level of theory, instead of the expected 81 structures. The side-chain conformers found for each backbone conformer is given in Figure 3. The DFT results of geometry optimizations of the title compound at the B3LYP/6-31G(*d*) level of theory, including geometrical parameters, total energies, relative energies, and stabilizations energies, are given in Table II. The total energies are given in hartree and relative and stabilization energies are given in kcal · mol^{-1} (using the conversion factor 1 hartree = 627,5095 kcal · mol^{-1}).

DFT calculations predict the $\gamma_L(g^-a)$ conformation as the global minimum. This backbone conformation is folded (C_7 form) and the side chain is partially folded. There are seven γ_L forms ($g^+g_1^+$, g^+a, ag^+, aa, g^-g^+, g^-a, and g^-g^-) and five β_L conformations (g^+a, ag^+, aa, g^-a, and g^-g^-) possessing energy gaps that were <2 kcal · mol^{-1} with respect to the global minimum. It is clear that DFT calculations predict the $\gamma_L(C_7)$ and $\beta_L(C_5)$ forms as the highly preferred conformations for the backbone of compound **I** in gas phase. Also, the low-energy gaps separating the different conformations suggest that a significant conformational interconversion can take place in this compound.

Examination of the relative energy differences obtained for the conformations of Ile allows a comparison between theoretical calculations reported here with previously reported experimental data obtained from x-ray [52–54] and nuclear magnetic resonance [55] studies. It is interesting to note that our theoretical calculations are in agreement with the experimental data.

In most peptides, all nine legitimate conformers will not appear as energy minima on the Ramachandran PES [4, 56, 57]. Most often, the α_L and ε_L conformations are annihilated [4, 56, 57]; however,

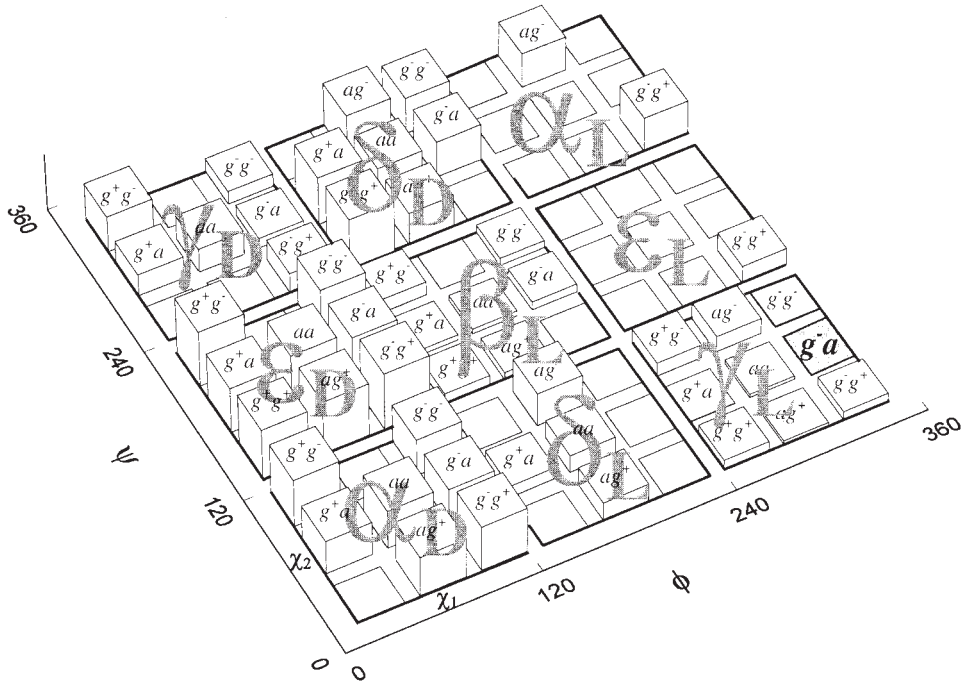

FIGURE 3. Schematic representation of the 53 existing minima on the PEHS of four independent variables: $E = E(\phi, \psi, \chi_1, \chi_2)$ for *N*-acetyl-L-isoleucine-*N*-methylamide obtained from B3LYP/6-31G(*d*) calculations. The global minimum, $\gamma_L(g^-a)$, is denoted in gray, and the energy gap above the global minimum is in relationship with the highest of the block.

for Glu[2], Gln[8], and Trp[58] the α_L conformation was reported as an energy minimum on the Ramachandran PES. Particularly noteworthy is the fact that, until now, Ile is the only reported amino acid that contains stable conformers at all nine backbone conformations at the DFT level of theory. Thus, both α_L and ε_L conformations, which are usually annihilated, are now energy minima on the Ramachandran PES. DFT [B3LYP/6-31G(*d*)] calculations predict the existence of two conformers $\alpha_L(ag^-)$ and $\alpha_L(g^-g^+)$. These forms possess 7.14 and 6.86 kcal · mol^{-1} above the global minimum, respectively. The same might be said for the ε_L backbone conformation. DFT calculations predict the existence of $\varepsilon_L(g^-g^+)$ conformation possessing 3.53 kcal · mol^{-1} above the global minimum.

As in all previous cases of L-amino acids studied, D-subscript conformers (α_D, ε_D, γ_D, and δ_D) are not preferred due to their relatively high energy values. However, for Ile, the $\gamma_D(g^-a)$ and $\gamma_D(g^-g^-)$ conformations display only 2.05 and 2.67 kcal · mol^{-1} above the global minimum, respectively. It should be noted that, practically, only destabilizing interactions (with positive ΔE_{stabil}) were found for compound **I** (Table II, last column). In fact, only some interactions for the γ_L and β_L forms possess negative values; however, these ΔE_{stabil} are small values ranging from −0.03 to −1.91 kcal · mol^{-1}. These results are in agreement with the high conformational inter-conversion found for compound **I**. The highest ΔE_{stabil} values were obtained for D-subscript conformers (α_D, δ_D, and γ_D), and consequently these forms are the less preferred conformations for compound **I**.

Considering an energy window of 5 kcal · mol^{-1}, there are 27 different conformations for **I**, indicating a remarkable conformational flexibility for this compound. It is clear that the weak molecular interactions stabilizing or destabilizing the different spatial orderings are of particular interest in this case. Thus, in the next section we performed a Bader analysis to obtain more precise information about the intramolecular interactions stabilizing the different spatial orientations adopted by compound **I**.

INTRAMOLECULAR INTERACTIONS

The different types of intramolecular hydrogen bonding (H—b), i.e., backbone/backbone (BB/BB) and side chain/backbone (SC/BB) may occur in the

TABLE II

Torsional angles[a] and total energy values for backbone and side-chain conformers of *N*-acetyl-L-isoleucine-*N*-methylamide optimized at the B3LYP/6-31G(*d*) level of theory.*

Final geometry	χ_1 (1-2-7-8)	χ_2 (2-7-8-9)	χ_3 (7-8-9-10)	χ_4 (2-7-11-12)	ϕ (1-2-3-20)	ψ (1-2-3-26)	ω_0 (1-2-20-21)	ω_1 (2-3-26-27)	Total energy (hartree)	$\Delta E_{rel.}$ (kcal · mol^{-1})	ΔE_{stabil} (γ_L) (kcal · mol^{-1})
$\alpha_D(g^+a)$	63.3	165.4	−58.2	66.4	51.0	39.1	168.1	−174.3	−613.7822744	6.93	5.02
$\alpha_D(g^+g^-)$	65.4	−87.7	−58.6	64.2	48.7	40.8	171.3	−173.8	−613.7776840	9.81	7.90
$\alpha_D(ag^+)$	−159.6	59.6	−68.5	65.5	50.6	41.0	167.2	−173.8	−613.7802340	8.21	6.30
$\alpha_D(aa)$	−158.5	164.9	−56.3	66.5	50.6	41.6	167.0	−173.6	−613.7805876	7.99	6.08
$\alpha_D(g^-g^+)$	−35.7	101.7	−56.5	65.8	58.2	41.7	171.0	−174.5	−613.7785403	9.27	7.36
$\alpha_D(g^-a)$	−36.4	177.2	−55.0	66.8	62.5	39.9	167.8	−175.0	−613.7820019	7.10	5.19
$\alpha_D(g^-g^-)$	−37.3	−62.9	−60.0	58.8	62.1	40.1	168.3	−174.9	−613.7812561	7.57	5.66
$\varepsilon_D(g^+g^+)$	54.0	74.6	−66.8	65.7	45.3	−146.4	−163.7	180.0	−613.7768255	10.35	8.44
$\varepsilon_D(g^+a)$	62.0	165.1	−58.5	64.1	45.2	−142.9	−164.2	179.7	−613.7785134	9.29	7.38
$\varepsilon_D(g^+g^-)$	60.0	−86.6	−61.4	61.7	43.4	−137.5	−163.5	177.2	−613.7750074	11.49	9.58
$\varepsilon_D(ag^+)$	−127.3	67.4	−60.7	70.5	73.9	164.4	−158.9	177.0	−613.7757909	11.00	9.09
$\varepsilon_D(aa)$	−128.0	171.6	−55.2	72.0	74.01	164.1	−158.7	177.1	−613.7758078	10.99	9.08
$\varepsilon_D(g^-g^+)$	−70.0	66.2	−69.6	61.1	76.8	137.9	−155.6	174.9	−613.7746472	11.71	9.80
$\varepsilon_D(g^-a)$	−55.8	163.9	−59.8	57.9	80.0	139.0	−156.7	175.2	−613.7780426	9.58	7.67
$\varepsilon_D(g^-g^-)$	−50.1	−58.6	−57.4	57.5	76.4	142.1	−170.8	176.5	−613.7773374	10.03	8.12
$\gamma_D(g^+a)$	73.1	167.7	−56.2	69.0	60.0	−32.5	173.9	−177.2	−613.7861240	4.51	2.60
$\gamma_D(g^+g^-)$	78.9	−84.0	−56.0	65.2	53.4	−31.3	174.4	−177.1	−613.7815812	7.36	5.45
$\gamma_D(aa)$	−149.3	173.3	−54.4	69.1	62.6	−37.5	173.4	−177.2	−613.7855530	4.87	2.96
$\gamma_D(g^-g^+)$	−65.2	71.7	−71.2	59.9	74.3	−62.0	175.8	178.1	−613.7868009	4.09	2.18
$\gamma_D(g^-a)$	−57.7	170.0	−57.1	60.3	73.8	−61.4	176.2	178.6	−613.7900467	2.05	0.14
$\gamma_D(g^-g^-)$	−26.6	−61.5	−58.0	57.5	73.6	−60.6	176.5	179.1	−613.7890543	2.67	0.76
$\delta_L(g^+a)$	61.7	169.0	−56.7	67.3	−121.2	18.0	−169.9	174.3	−613.7894745	2.41	0.50
$\delta_L(ag^+)$	−162.4	55.5	−69.8	66.0	−123.3	14.8	−168.8	174.4	−613.7876484	3.56	1.65
$\delta_L(aa)$	−159.4	167.3	−55.7	67.6	−130.4	21.6	−168.6	174.2	−613.7876794	3.54	1.63
$\delta_L(ag^-)$	−143.7	−76.6	−59.2	66.1	−128.3	19.2	−168.1	174.6	−613.7825519	6.75	4.84
$\beta_L(g^+g^+)$	54.0	73.0	−66.9	66.8	−129.5	164.4	168.9	179.4	−613.7898200	2.19	0.28
$\beta_L(g^+a)$	60.1	169.8	−57.4	66.4	−130.3	159.9	168.8	178.4	−613.7915311	1.12	−0.79
$\beta_L(g^+g^-)$	76.4	−62.0	−51.9	67.7	−131.1	159.1	169.8	177.9	−613.7888059	2.83	0.92
$\beta_L(ag^+)$	−167.6	59.7	−67.4	68.0	−152.2	173.2	176.5	−163.4	−613.7909705	1.47	−0.44
$\beta_L(aa)$	−167.2	165.1	−56.9	68.5	−152.8	153.3	176.6	177.9	−613.7916909	1.02	−0.89
$\beta_L(g^-a)$	−58.5	169.8	−56.8	61.3	−123.9	131.1	172.7	179.7	−613.7906880	1.65	−0.26
$\beta_L(g^-g^-)$	−55.4	−63.9	−58.0	58.6	−121.4	131.4	172.7	179.7	−613.7909037	1.51	−0.40
$\delta_D(g^+g^+)$	8.1	69.4	−68.8	63.3	−152.9	−50.2	167.3	−174.0	−613.7767295	10.41	8.50
$\delta_D(g^+a)$	24.2	166.4	−57.3	63.4	−163.9	−41.2	165.8	−172.5	−613.7776288	9.84	7.93
$\delta_D(ag^+)$	−175.2	57.0	−70.9	71.0	−160.1	−37.2	168.8	−174.4	−613.7826199	6.71	4.80

(*continued*)

TABLE II
(Continued)

Final geometry	χ_1 (1-2-7-8)	χ_2 (2-7-8-9)	χ_3 (7-8-9-10)	χ_4 (2-7-11-12)	ϕ (1-2-3-20)	ψ (1-2-3-26)	ω_0 (1-2-20-21)	ω_1 (2-3-26-27)	Total energy (hartree)	$\Delta E_{rel.}$ (kcal · mol^{-1})	ΔE_{stabil} (γ_L) (kcal · mol^{-1})
$\delta_D(aa)$	−171.7	168.3	−56.1	72.0	−160.2	−37.4	168.3	−174.4	−613.7824228	6.83	4.93
$\delta_D(ag^-)$	−164.6	−76.5	−58.3	69.5	−154.7	−45.2	169.8	−175.5	−613.7794089	8.73	6.82
$\delta_D(g^-a)$	−58.1	172.8	−56.1	63.0	−126.0	−66.7	169.7	−177.1	−613.7815250	7.40	5.49
$\delta_D(g^-g^-)$	−57.7	−65.9	−58.4	57.2	−122.0	−67.0	171.1	−177.5	−613.7813135	7.53	5.62
$\gamma_L(g^+g^+)_1$	42.1	55.3	−64.9	61.2	−83.2	54.3	−173.8	177.0	−613.7903215	1.88	−0.03
$\gamma_L(g^+g^+)_2$	50.8	57.6	−65.9	63.2	−118.1	15.8	−170.1	173.1	−613.7883263	3.13	1.22
$\gamma_L(g^+a)$	53.6	161.0	−60.6	61.5	−83.3	65.8	−176.8	−178.2	−613.7930344	0.18	−1.73
$\gamma_L(g^+g^-)_1$	67.7	−64.7	−48.7	65.4	−84.5	63.2	−174.1	−179.0	−613.7888463	2.80	0.89
$\gamma_L(g^+g^-)_2$	77.0	−59.4	−52.1	69.0	−118.8	10.6	−170.2	173.8	−613.7865019	4.27	2.37
$\gamma_L(ag^+)$	−175.1	56.5	−67.5	61.5	−84.0	74.1	−177.4	−175.1	−613.7922609	0.66	−1.25
$\gamma_L(aa)$	−172.8	164.9	−56.8	62.5	−84.1	71.5	−177.0	−175.9	−613.7921951	0.70	−1.21
$\gamma_L(ag^-)$	−161.5	−67.2	−53.8	64.3	−83.4	80.4	−178.4	−172.7	−613.7881349	3.25	1.34
$\gamma_L(g^-g^+)$	−50.5	92.1	−66.4	64.6	−83.1	79.1	179.4	−173.4	−613.7907810	1.59	−0.32
$\gamma_L(g^-a)$	−53.5	171.0	−56.7	62.3	−83.5	80.1	180.0	−172.9	−613.7933138	**0.00**	−1.91
$\gamma_L(g^-g^-)$	−50.6	−61.4	−59.0	57.9	−84.5	79.2	−178.8	−173.4	−613.7928342	0.30	−1.61
$\varepsilon_L(g^-g^+)$	−77.8	59.6	−70.5	60.0	−112.8	130.5	170.8	−179.5	−613.7876847	3.53	1.62
$\alpha_L(ag^-)$	−162.1	−86.2	−60.1	63.5	−78.6	−25.0	−168.1	175.0	−613.7819371	7.14	5.23
$\alpha_L(g^-g^+)$	−84.3	58.8	−64.7	57.7	−78.1	−28.2	−170.1	174.7	−613.7823837	6.86	4.95

* The calculated relative energies (ΔE_{rel})[b] and stabilization energies (ΔE_{stabil}) values are also shown.
[a] Torsional angles in deg.
[b] The global minimum corresponds to the $\gamma_L(g^-a)$ conformation having a total energy of −613.7933138 hartree. This value is taken as a reference value, corresponding to a relative energy value of 0.00 kcal · mol^{-1}.

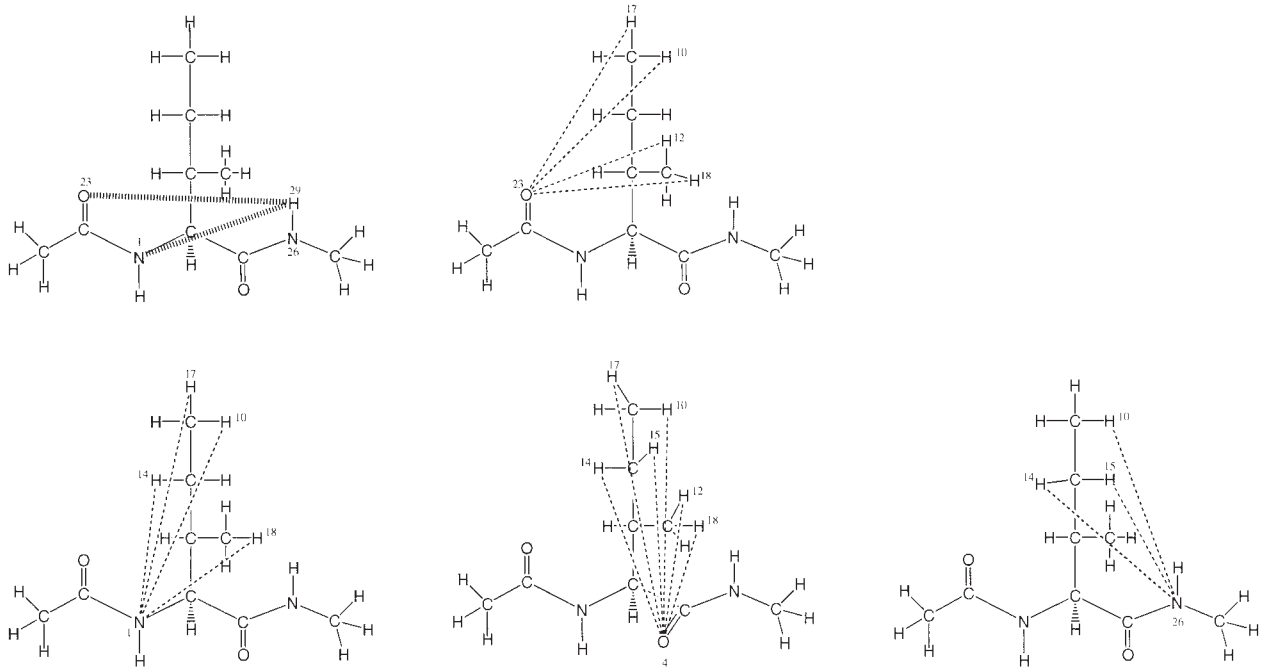

FIGURE 4. Schematic representation of the different types of intramolecular hydrogen bondings of the most representative conformations of *N*-acetyl-L-isoleucine-*N*-methylamide. Backbone/backbone (B/B) interactions are denoted by (IIII), and side-chain/backbone (SC/BB) interactions are denoted by (– – –).

different conformations of compound **I** are depicted in Figure 4.

An alternative method to analyze hydrogen bonding involves the topological analysis of electronic density distribution, which can be used to analyze intramolecular hydrogen bonding between H and a nearby heteroatom (Y) to gain some insight into the effect of hydrogen bond interactions on the conformations of amino acids.

Table III displays the most significant topological local properties: electronic density (ρ_b), Laplacian of the electronic density ($\nabla^2\rho_b$) and ellipticity (ε) at the bond critical points (3, −1) for the most representative structures obtained for Ile. The topological local properties reported in this study correspond to the bond critical points from X—H…Y, where H represents the hydrogen atom involved in the bond. We discuss only the most representative conformations. These results account for the general characteristics of the electronic behavior of Ile. However, computations have been carried out for the rest of conformations of compound **I** with these results being considered representative of the overall phenomenon (Supplementary Material, Table IS).

A strong N—H…O hydrogen bond (the so-called C_7) is stabilizing all the γ_L conformations, except the $\gamma_L(g^+g^+)_2$ and $\gamma_L(g^+g^-)_2$ conformations that displayed higher energy compared with the other conformers of this backbone type (ΔE = 3.13 kcal · mol^{-1} and ΔE = 4.27 kcal · mol^{-1}, respectively).

The low-energy forms $\gamma_L(g^-a)$, $\gamma_L(g^+a)$, and $\gamma_L(g^-g^-)$ have only two hydrogen bonds: a strong one between N_{26}—H_{29}…O_{23} (BB/BB) and a weak bond C—H…O (SC/BB) (Table III). The BB/BB interactions in these three minimum-energy conformations have very similar topological properties. The values of ρ_b range from 0.0182 to 0.0217 a.u., and the values of $\nabla^2\rho_b$ range from 0.0713 to 0.877 a.u. These bonds are stable, having a low value of ellipticity (ε) close to 0.06. In contrast, the weak bond C—H…O (SC/BB) has lower values of ρ_b (from 0.0102 to 0.0114 a.u.) and $\nabla^2\rho_b$ (from 0.0391 to 0.0417 a.u.).

The $\gamma_L(ag^+)$ and $\gamma_L(aa)$ conformations possess four monodirectional H—b's: N_{26}—H_{29}…O_{23} (BB/BB), C_{11}—H_{18}…N_1 (SC/BB), C_{11}—H_{12}…O_4 (SC/BB), and C_8—$H_{14(15)}$…O_4 (SC/BB). It should be noted that the two last ones are bifurcated H—b's (Fig. 5). All these interactions participate in the definition of five topological rings [five ring critical points or (3, +1) points] probably stabilizing these

TABLE III

Topological properties[a] at hydrogen bond critical points of the most representative structures for *N*-acetyl-L-Isoleucine-*N*-methylamide [RHF/6-311++G(*d*,*p*)//6-31G(*d*)].*

Conformers	Involved atoms	$\rho(r_b)$	$\nabla^2\rho(r_b)$	ε	Distance H…Y (Å)	Angle X—H…Y (°)
$\gamma_L(g^-a)$	N_{26}—H_{29}…O_{23}	0.0182	0.0713	0.0648	2.867	91.2
	C_{11}—H_{18}…O_4	0.0106	0.0410	0.6271	2.517	116.1
$\gamma_L(g^+a)$	N_{26}—H_{29}…O_{23}	0.0217	0.0877	0.0608	2.007	148.3
	C_8—H_{14}…O_4	0.0114	0.0417	0.2335	2.461	108.6
$\gamma_L(g^-g^-)$	N_{26}—H_{29}…O_{23}	0.0182	0.0717	0.0623	2.100	142.1
	C_{11}—H_{18}…O_4	0.0102	0.0391	0.5593	2.538	115.2
$\gamma_L(ag^+)$	N_{26}—H_{29}…O_{23}	0.0206	0.0823	0.0598	2.038	145.7
	C_{11}—H_{12}…O_4	0.0123	0.0450	0.1678	2.408	118.7
	C_{11}—H_{18}…N_1	0.0104	0.0432	1.3105	2.750	93.5
	C_8—H_{14}…O_4	0.0098	0.0355	0.3681	2.548	116.6
$\gamma_L(aa)$	N_{26}—H_{29}…O_{23}	0.0212	0.0853	0.0594	2.021	146.6
	C_{11}—H_{12}…O_4	0.0126	0.0461	0.1615	2.397	118.6
	C_8—H_{15}…O_4	0.0099	0.0358	0.3328	2.544	115.5
	C_{11}—H_{18}…N_1	0.0104	0.0427	1.2242	2.747	94.4
$\gamma_L(ag^-)$	N_{26}—H_{29}…O_{23}	0.0192	0.0757	0.0609	2.077	142.9
	C_{11}—H_{12}…O_4	0.0137	0.0511	0.1378	2.363	116.1
	C_9—H_{17}…O_4	0.0078	0.0298	1.0634	2.779	102.9
$\gamma_L(g^+g^+)_2$	N_{26}—H_{29}…N_1	0.0183	0.0795	0.7895	2.271	107.2
$\gamma_L(g^+g^-)_2$	N_{26}—H_{29}…N_1	0.0187	0.0805	0.6962	2.258	107.5
	C_9—H_{10}…N_1	0.0100	0.0388	0.3500	2.835	101.5
	C_8—H_{15}…O_4	0.0090	0.0367	2.8392	2.614	115.2
$\gamma_L(g^+g^+)_1$	N_{26}—H_{29}…O_{23}	0.0229	0.0929	0.0633	1.980	150.8
	C_8—H_{14}…N_1	0.0119	0.0529	2.3672	2.754	88.3
	C_9—H_{17}…O_4	0.0089	0.0329	0.3169	2.613	107.6
$\gamma_L(g^+g^-)_1$	N_{26}—H_{29}…O_{23}	0.0227	0.0920	0.0593	1.986	149.5
	C_8—H_{15}…O_4	0.0147	0.0546	0.1315	2.311	121.5
	C_9—H_{17}…N_1	0.0121	0.0474	0.3408	2.797	101.0
$\gamma_L(g^-g^+)$	N_{26}—H_{29}…O_{23}	0.0180	0.0705	0.0652	2.107	141.9
	C_{11}—H_{18}…O_4	0.0097	0.0406	3.4202	2.583	114.2
	C_9—H_{10}…N_1	0.0095	0.0344	0.5631	2.678	112.5
$\beta_L(g^+g^+)$	C_{11}—H_{12}…O_{23}	0.0055	0.0228	1.3793	2.904	101.9
	C_9—H_{10}…O_4	0.0099	0.0337	0.6083	2.500	139.5
$\beta_L(g^+a)$	C_{11}—H_{18}…O_{23}	0.0048	0.0204	1.5745	2.999	100.2
$\beta_L(g^+g^-)$	C_{11}—H_{18}…O_{23}	0.0061	0.0223	0.0821	2.792	111.6
	C_9—H_{17}…O_4	0.0057	0.0199	0.1549	2.787	126.4
	C_9—H_{17}…N_1	0.0068	0.0272	1.1659	2.810	104.4
$\beta_L(ag^+)$	C_8—H_{14}…N_{26}	0.0084	0.0282	0.1284	2.733	112.1
	C_9—H_{10}…N_{26}	0.0048	0.0178	0.3360	3.231	111.4
$\beta_L(aa)$	C_8—H_{15}…N_{26}	0.0082	0.0285	0.2453	2.768	107.6
$\beta_L(g^-a)$	—	—	—	—	—	—
$\beta_L(g^-g^-)$	C_9—H_{17}…O_{23}	0.0079	0.0259	0.0754	2.565	145.2
$\alpha_L(ag^-)$	C_9—H_{17}…O_4	0.0140	0.0505	0.0311	2.279	136.8
	N_{26}—H_{29}…N_1	0.0181	0.0781	0.9116	2.278	107.7
$\alpha_L(g^-g^+)$	N_{26}—H_{29}…N_1	0.0178	0.0767	1.0379	2.291	107.5
	C_9—H_{10}…N_1	0.0093	0.0329	0.2590	2.706	103.9
$\varepsilon_L(g^-g^+)$	C_9—H_{10}…N_1	0.0086	0.0327	0.8147	2.743	101.5
	C_9—H_{10}…O_{23}	0.0082	0.0286	0.7405	2.572	149.9

* Covalent bonds are denoted as X—H and hydrogen bonds specified as H…Y.

[a] All values are expressed in a.u.

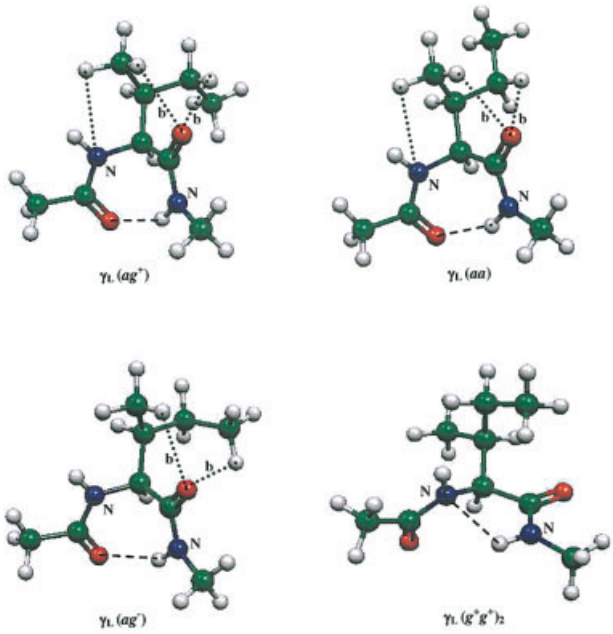

FIGURE 5. Spatial views of the most representative geometries of *N*-acetyl-L-isoleucine-*N*-methylamide showing different hydrogen bondings (H-b). Bifurcated H-b are denoted by (**b**).

two conformations, which are 0.66 and 0.70 kcal · mol^{-1} above the global minimum, respectively. In contrast, the $\gamma_L(ag^-)$ form displays only three monodirectional H—b's: N_{26}—H_{29}…O_{23} (BB/BB), C_{11}—H_{12}…O_4 (SC/BB), C_9—H_{17}…O_4 (SC/BB), since the C_{11}—H_{18}…N_1 (SC/BB) interaction is missing. As a consequence, only four topological rings probably destabilizing this conformation are defined (ΔE = 3.25 kcal · mol^{-1}).

The hydrogen bonding N_{26}—H_{29}…N_1 that is, a BB/BB interaction is holding the backbone in only two γ_L conformations: the $\gamma_L(g^+g^+)_2$ (Fig. 5) and $\gamma_L(g^+g^-)_2$ forms. The high values of ε found in these two conformations are in agreement with the low values of ρ_b (0.0183 and 0.0187 a.u.). These values of ellipticity predict that these bonds are unstable, very close to breaking. This is also in agreement with bond angles of 107.2° and 107.5°, which are closer to 90° rather than 180°. The presence of these weak interactions, instead of the typical strong C_7 hydrogen bond, should explain the low stability of these two conformers.

An interesting observation can be made with respect to the β_L conformations from the topological analysis. All the β_L forms display only weak hydrogen bonds C—H…O and C—H…N, with high values of ellipticity and low values of density and Laplacian (Table III). These results might indicate why the β_L conformations are slightly disfavored compared with the γ_L forms.

The α_L and ε_L forms that are usually annihilated are now energy minima on the Ramachandran PES of **I**. The $\alpha_L(g^-g^+)$ form displays interesting stabilizing interactions: N_{26}—H_{29}…N_1 (BB/BB) and C_9—H_{10}…N_1 (SC/BB). It should be noted that these two interactions form a bifurcated H—b. The $\varepsilon_L(g^-g^+)$ conformation has two weak monodirectional H—b's: C_9—H_{10}…N_1 (SC/BB) and C_9—H_{10}…O_{23} (SC/BB).

According to the results of Bader analysis and taking into account that Ile has an apolar side chain, it appears that backbone interactions N—H_{BB}…O_{BB} are most significant in stabilizing the γ_L conformations. Thus, the conformations showing other types of interactions, i.e., N—H_{BB}…N_{BB}, C—H_{SC}…N_{BB}, and C—H_{SC}…O_{BB}, have lower stability.

EFFECT OF SOLVENT

Theoretical studies of solvent effects on large and medium-size molecules are currently proceeding mainly from two points of view: the continuum model and the supermolecule model. In the continuum model, a solute molecule is treated explicitly with the solvent represented as a polarizable dielectric continuum, which modulates intramolecular solute interactions, interacts with a solute molecule via induced electric fields, or both. The continuum model has its origins in classical electrostatic treatments of interacting systems and the work of Born [59], Onsager [60], and Kirkwood [61].

The supermolecule approach involves explicitly including one or more solvent molecules in the calculation, and determining conformational energies and related properties for the assembly.

The supermolecule model has the capability of dealing with certain problems where the continuum model is inadequate but suffers from limitations of different sort. Most solvation site studies are carried out considering explicitly the solute molecules and one or two waters of hydration. The sensitivity of these results to inclusion of additional solvent molecules is a factor to contend with. Cooperative effects among a number of solvent molecules arise as a common feature in biological systems possessing medium-size apolar side chains. Thus, Ile will not be amenable to the supermolecule approach unless a laborious geometry optimization explicitly including numerous solute molecules was previously carried out. However, caution is

also necessary for the use of the continuum model approach for Ile. Particular care should be exercised in the application of the continuum model to solvent effects in problems involving the stabilization of certain conformations by intramolecular hydrogen bonding [22]. Because the solvent lacks structure in this model, it is not appropriate for solvents that have important specific interactions (e.g., hydrogen bonds) with the solute. It does, however, have the advantage of allowing the geometry and dipole moment of the solute to be adjusted to reflect the interactions with the medium.

Under these conditions, we have adopted the IPCM approach [22]. We do not expect the entire solution behavior of Ile to be explained by such a reduced treatment. Our aim in this study is less ambitious: we wish to obtain a reasonable indication of the direction and magnitude of changes in conformational preferences of the isolated molecule when it enters different solutions, and from this point of view the inclusion in the computations of three solvents with different dielectric constants should be particularly significant.

According to the results of IPCM calculations shown in Table IV and Figure 6, it is clear that the conformational preferences of Ile are different in vacuo than are in solution.

Although the observed solvent effects depend somewhat on the solvent nature, the β_L, α_L, and γ_D conformations are commonly stabilized in solution, irrespective of the solvent type. In contrast, the γ_L backbone conformations are in general disfavored by the effects of solvent. It is also notable that the effects of solvent polarity are rather small, at least in the range of 4.9 (chloroform) $\leq \varepsilon \leq$ 78.39 (water), compared with the larger solvent effects observed by changing the medium from vacuum ($\varepsilon = 1.0$) to chloroform ($\varepsilon = 4.9$).

It is interesting to note that the $\gamma_L(g^-a)$ conformation, which is the global minimum in vacuo, possesses 1.80 kcal $\cdot$ mol^{-1} above the global minimum in water, being the ninth local minimum in energy in this solvent. The $\gamma_D(g^-a)$ form possessing 2.05 kcal $\cdot$ mol^{-1} above the global minimum in vacuo displays an energy gap of only 0.73 kcal $\cdot$ mol^{-1} in water, being the fifth local minimum. The most abrupt change observed corresponds to $\alpha_L(g^-g^+)$ form. This conformation possesses 6.86 kcal $\cdot$ mol^{-1} above the global minimum in vacuo, but the energy gap is reduced to 2.28 kcal $\cdot$ mol^{-1} in water. These results are in agreement with those previously reported for Gly and Ala by Head-Gordon and colleagues [62, 63] (using the simple Onsager's dipole model) and Tomoda and colleagues [49] (using PCM and IPCM methods). They reported that stable conformers were located in vacuo only in the regions of $C_5(\beta_L)$ and $C_7(\gamma_L)$; however, these conformers were relatively destabilized in the IPCM potential obtained in water. Instead, stable energy minima appeared in the regions of α, PII, and β_2. They suggest that the intramolecular hydrogen bonds present in the γ_L and β_L forms are strong in vacuo but are weak in polar environments. Our results are in complete agreement with those of Head-Gordon and Tomada. Although for Ile the $\beta_L(C_5)$ forms are the preferred conformations in the three solvents, it should be noted that BADER analysis indicates that there are no strong hydrogen bonds stabilizing these conformations. Head-Gordon and Tomada also reported that the conformational space of Gly and Ala are more restricted in water that in vacuo. On the basis of our results, we cannot say the same for Ile. Considering an energy window of 5 kcal $\cdot$ mol^{-1}, 27 different conformations were obtained in vacuo, whereas 26 different forms were found in water and acetonitrile. In the case of chloroform, 30 different conformations were obtained for Ile which possessed an energy gap of $<$5 kcal $\cdot$ mol^{-1}. There are several explanations for these results. One possibility is that these could be a manifestation of the key role played by the apolar side chain (hydrophobic effects) in the conformational interconversions of Ile. Another possible contributing factor could be the higher conformational flexibility observed in Ile in comparison with those of Gly and Ala.

Conclusions

The full conformational space of *N*-acetyl-L-isoleucine-*N*-methylamide was explored by DFT [B3LYP/6-31G(*d*)] computations. On the Ramachandran hypersurface of four independent variables $E = E(\phi, \psi, \chi_1, \chi_2)$, 53 conformers were located instead of the $3^4 = 81$ stable structures. DFT calculations predict the $\gamma_L(C_7)$ and $\beta_L(C_5)$ forms as the highly preferred conformations for the backbone of compound **I** in the gas phase. IPCM/B3LYP/6-31G(*d*) calculations indicate that the γ_L backbone conformations possessing a strong internal hydrogen bond are disfavored by the effects of the solvent irrespective of the solvent type. In contrast, the β_L, and particularly the α_L forms were significantly favored by effects of the solvents.

TABLE IV

Calculated relative energies[a] for all the conformations of *N*-acetyl-L-isoleucine-*N*-methylamide obtained in gas phase and in three different solvents.*

Conformation	B3LYP/6-31G(*d*) gas phase (ΔE_{rel})	Conformation	IPCM/B3LYP/6-31G(*d*) chloroform (ΔE_{rel})	Conformation	IPCM/B3LYP/6-31G(*d*) acetonitrile (ΔE_{rel})	Conformation	IPCM/B3LYP/6-31G(*d*) water (ΔE_{rel})
$\gamma_L(g^-a)$	**0.00**	$\beta_L(ag^+)$	**0.00**	$\beta_L(ag^+)$	**0.00**	$\beta_L(ag^+)$	**0.00**
$\gamma_L(g^+a)$	0.18	$\beta_L(g^-a)$	0.08	$\beta_L(g^-a)$	0.20	$\beta_L(g^-a)$	0.24
$\gamma_L(g^-g^-)$	0.30	$\beta_L(aa)$	0.17	$\gamma_D(g^-a)$	0.36	$\gamma_D(g^-a)$	0.26
$\gamma_L(ag^+)$	0.66	$\gamma_L(g^-g^-)$	0.26	$\beta_L(aa)$	0.49	$\beta_L(aa)$	0.52
$\gamma_L(aa)$	0.70	$\gamma_L(g^-a)$	0.53	$\gamma_D(g^-g^-)$	0.76	$\gamma_D(g^-g^-)$	0.73
$\beta_L(aa)$	1.02	$\beta_L(g^-g^-)$	0.70	$\gamma_L(g^-g^-)$	1.25	$\gamma_L(g^-g^-)$	1.36
$\beta_L(g^+a)$	1.12	$\gamma_D(g^-a)$	0.73	$\beta_L(g^-g^-)$	1.31	$\beta_L(g^-g^-)$	1.39
$\beta_L(ag^+)$	1.47	$\beta_L(g^+a)$	0.82	$\beta_L(g^+a)$	1.59	$\beta_L(g^+a)$	1.68
$\beta_L(g^-g^-)$	1.51	$\gamma_D(g^-g^-)$	1.00	$\gamma_L(g^-a)$	1.67	$\gamma_L(g^-a)$	1.80
$\gamma_L(g^-g^+)$	1.59	$\gamma_L(ag^+)$	1.22	$\gamma_L(ag^+)$	2.03	$\gamma_L(ag^+)$	2.12
$\beta_L(g^-a)$	1.65	$\gamma_L(g^+g^+)_1$	2.07	$\delta_L(aa)$	2.24	$\delta_L(aa)$	2.22
$\gamma_L(g^+g^+)_1$	1.88	$\gamma_L(g^-g^+)$	2.23	$\alpha_L(g^-g^+)$	2.40	$\alpha_L(g^-g^+)$	2.28
$\gamma_D(g^-a)$	2.05	$\gamma_L(aa)$	2.23	$\gamma_L(g^+g^-)_2$	2.75	$\gamma_L(g^+g^-)_2$	2.73
$\beta_L(g^+g^+)$	2.19	$\delta_L(aa)$	2.35	$\gamma_L(g^+g^+)_1$	2.96	$\gamma_L(g^+g^+)_1$	3.06
$\delta_L(g^+a)$	2.41	$\delta_L(g^+a)$	2.38	$\varepsilon_L(g^-g^+)$	3.09	$\alpha_D(g^-g^-)$	3.07
$\gamma_D(g^-g^-)$	2.67	$\varepsilon_L(g^-g^+)$	2.52	$\gamma_L(g^+g^+)_2$	3.22	$\varepsilon_L(g^-g^+)$	3.16
$\gamma_L(g^+g^-)_1$	2.80	$\beta_L(g^+g^+)$	2.66	$\alpha_D(g^-g^-)$	3.30	$\gamma_L(g^+g^+)_2$	3.28
$\beta_L(g^+g^-)$	2.83	$\gamma_L(g^+g^+)_2$	2.71	$\gamma_L(g^-g^+)$	3.47	$\delta_D(g^-a)$	3.41
$\gamma_L(g^+g^+)_2$	3.13	$\gamma_L(g^+g^-)_2$	2.89	$\delta_D(g^-a)$	3.51	$\gamma_L(g^-g^+)$	3.61
$\gamma_L(ag^-)$	3.25	$\alpha_L(g^-g^+)$	3.45	$\beta_L(g^+g^+)$	3.60	$\beta_L(g^+g^+)$	3.70
$\varepsilon_L(g^-g^+)$	3.53	$\gamma_D(g^-g^+)$	3.71	$\gamma_L(aa)$	3.64	$\gamma_L(aa)$	3.79
$\delta_L(aa)$	3.54	$\gamma_L(g^+g^-)_1$	4.06	$\delta_D(ag^+)$	4.09	$\delta_D(ag^+)$	3.94
$\delta_L(ag^+)$	3.56	$\gamma_D(aa)$	4.33	$\gamma_D(g^+g^-)$	4.20	$\gamma_D(g^+g^-)$	4.13
$\gamma_D(g^-g^+)$	4.09	$\delta_D(g^-a)$	4.43	$\gamma_D(g^-g^+)$	4.43	$\gamma_D(g^-g^+)$	4.52
$\gamma_L(g^+g^-)_2$	4.27	$\gamma_D(g^+a)$	4.52	$\gamma_D(aa)$	4.81	$\gamma_D(aa)$	4.87
$\gamma_D(g^+a)$	4.51	$\gamma_L(ag^-)$	4.54	$\gamma_D(g^+a)$	4.95	$\gamma_D(g^+a)$	4.98
$\gamma_D(aa)$	4.87	$\beta_L(g^+g^-)$	4.65	$\delta_D(aa)$	5.09	$\delta_D(aa)$	5.03
$\delta_D(ag^+)$	6.71	$\gamma_D(g^+g^-)$	4.89	$\gamma_L(g^+g^-)_1$	5.29	$\alpha_D(aa)$	5.17
$\delta_L(ag^-)$	6.75	$\delta_D(ag^+)$	4.96	$\alpha_D(aa)$	5.29	$\alpha_D(ag^+)$	5.26
$\delta_D(aa)$	6.83	$\alpha_D(g^-g^-)$	4.98	$\alpha_D(ag^+)$	5.37	$\gamma_L(g^+g^-)_1$	5.41
$\alpha_L(g^-g^+)$	6.86	$\alpha_D(aa)$	5.42	$\gamma_L(ag^-)$	5.75	$\alpha_D(g^-a)$	5.70
$\alpha_D(g^+a)$	6.93	$\alpha_L(ag^-)$	6.00	$\alpha_D(g^-a)$	5.75	$\alpha_L(ag^-)$	5.79
$\alpha_D(g^-a)$	7.10	$\alpha_D(g^-a)$	6.10	$\alpha_L(ag^-)$	5.83	$\varepsilon_D(g^-g^+)$	5.85
$\alpha_L(ag^-)$	7.14	$\alpha_D(aa)$	6.16	$\alpha_D(g^-g^+)$	5.99	$\gamma_L(ag^-)$	5.87
$\gamma_D(g^+g^-)$	7.36	$\alpha_D(ag^+)$	6.23	$\varepsilon_D(g^-g^+)$	6.09	$\alpha_D(g^-g^+)$	5.87
$\delta_D(g^-a)$	7.40	$\alpha_D(g^+a)$	6.72	$\beta_L(g^+g^-)$	6.47	$\varepsilon_D(g^+a)$	6.52
$\delta_D(g^-g^-)$	7.53	$\delta_D(ag^-)$	6.96	$\varepsilon_D(g^+a)$	6.58	$\beta_L(g^+g^-)$	6.66
$\alpha_D(aa)$	7.99	$\varepsilon_D(g^+a)$	7.05	$\alpha_D(g^+a)$	7.23	$\alpha_D(g^+a)$	7.28
$\alpha_D(ag^+)$	8.21	$\varepsilon_D(g^-g^-)$	8.09	$\varepsilon_D(g^-g^-)$	7.55	$\varepsilon_D(g^-g^-)$	7.48
$\delta_D(ag^-)$	8.73	$\varepsilon_D(g^-g^+)$	8.09	$\delta_D(g^+g^+)$	8.72	$\delta_D(g^+g^+)$	8.70
$\alpha_D(g^-g^+)$	9.27	$\varepsilon_D(g^-a)$	8.81	$\varepsilon_D(ag^+)$	8.79	$\varepsilon_D(ag^+)$	8.74
$\varepsilon_D(g^+a)$	9.29	$\delta_D(g^+g^+)$	8.84	$\varepsilon_D(g^-a)$	8.95	$\varepsilon_D(g^-a)$	8.96
$\varepsilon_D(g^-a)$	9.58	$\delta_D(g^+a)$	9.06	$\delta_D(g^+a)$	9.34	$\delta_D(g^+a)$	9.37
$\alpha_D(g^+g^-)$	9.81	$\varepsilon_D(ag^+)$	9.21	$\varepsilon_D(aa)$	9.39	$\varepsilon_D(aa)$	9.63
$\delta_D(g^+a)$	9.84	$\alpha_D(g^+g^-)$	9.41	$\alpha_D(g^+g^-)$	9.85	$\alpha_D(g^+g^-)$	9.87
$\varepsilon_D(g^-g^-)$	10.03	$\varepsilon_D(g^+g^+)$	9.57	$\varepsilon_D(g^+g^+)$	9.85	$\varepsilon_D(g^+g^+)$	9.88
$\varepsilon_D(g^+g^+)$	10.35	$\varepsilon_D(aa)$	9.91	$\varepsilon_D(g^+g^-)$	10.93	$\varepsilon_D(g^+g^-)$	10.97
$\delta_D(g^+g^+)$	10.41	$\varepsilon_D(g^+g^-)$	10.60				
$\varepsilon_D(aa)$	10.99						
$\varepsilon_D(ag^+)$	11.00						
$\varepsilon_D(g^+g^-)$	11.49						
$\varepsilon_D(g^-g^+)$	11.71						

* A 2-kcal · mol^{-1} energy window is shown by broken lines.

[a] Relative energies in kcal · mol^{-1}; total energies values are available as Supplementary Material (Table IIS).

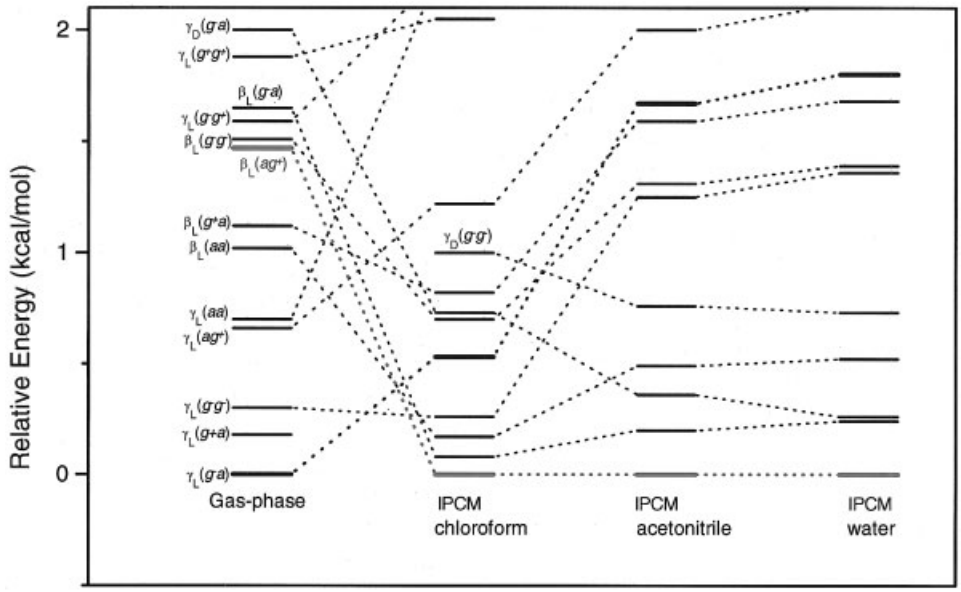

FIGURE 6. Energy window of 2 kcal · mol^{-1} showing the relative energies of *N*-acetyl-L-isoleucine-*N*-methylamide conformations obtained using B3LYP/6-31G(*d*) and IPCM/B3LYP/6-31G(*d*) calculations. Three different solvents were calculated (chloroform, acetonitrile, and water).

The electronic study of *N*-acetyl-L-isoleucine-*N*-methylamide was carried out using the AIM method. Using topological analysis, we found that N—H_{BB}…N_{BB}, C—H_{SC}…N_{BB}, and C—H_{SC}…O_{BB} have lower stability. On the basis of our results, it appears that the Bader-type analysis can contribute to a better understanding of some less noticeable electronic effects, which might influence the structure of a polypeptide or a protein possessing this residue in the structure.

Comparing the results obtained for **I** with other previously reported amino acids, a higher molecular flexibility was observed for this compound. Particularly noteworthy was the fact that **I** was the only amino acid, reported until now, possessing all nine different types of backbone conformations. Thus, the right-handed helix (α_L) and polyproline II (ε_L) conformations, which are usually annihilated, are now stable energy minima on the Ramachandran PES. We consider that the conformational intricacies of **I** should presumably be the result of stabilizing or destabilizing effects of its side chain. The results obtained for the right-handed helix (α_L) conformations of **I** compared with those attained previously for glutamate [2], glutamine [8], and aspartic acid [69] offer new insight into the influence of ionic and nonionic (polar or apolar) side chains on the conformational preferences of peptide structures. For glutamate and aspartic acid, the α_L is one of the preferred forms, whereas for isoleucine and glutamine, these forms possess 6.86 kcal · mol^{-1} and 5.1 kcal · mol^{-1} above the global minimum, respectively. It should be noted that the energy gap obtained for the $\alpha_L(g^-g^+)$ conformation of Ile in water was significantly lower than in the gas phase, being only 2.28 kcal · mol^{-1} in water. Also, it is clear that the size of the side chain that stabilizes α_L conformations is mandatory. This is particularly apparent, considering that for formyl-L-valinamide [9] and Ala [56], the α_L conformations were annihilated on the Ramachandran PES. Thus, it can be concluded that the insertion of a nonpolar side chain (e.g., that of Ile) into a peptide structure is not conformationally neutral and produces significant changes in the peptide structure. The effects of relatively long apolar side chain are very important to determine the conformational preferences of this compound.

ACKNOWLEDGMENTS

R. D. Enriz and N. M. Peruchena are members of career researcher of CONICET-Argentina. The authors thank Marco W. Klipfel for his help with the IPCM computations.

References

1. Fasman, G. D. Prediction of Protein Structure and Principles of Protein Conformations; Plenum: New York, 1989.
2. Masman, M. F.; Zamora, M. A.; Rodríguez, A. M.; Fidanza, N. G.; Peruchena, N. M.; Enriz, R. D.; Csizmadia, I. G. Eur Phys J D 2002, 20, 531.
3. Salpietro, S. J.; Perczel, A.; Farkas, O.; Enriz, R. D.; Csizmadia, I. G. J Mol Struct (Theochem) 2000, 497, 39.
4. Perczel, A.; Csizmadia, I. G. Int Rev Phys Chem 1995, 14, 127.
5. Zamora, M. A.; Baldoni, H. A.; Bombasaro, J. A.; Mak, M. L.; Perczel, A.; Farkas, O.; Enriz, R. D. J Mol Struct (Theochem) 2001, 540, 271.
6. Zamora, M. A.; Baldoni, H. A.; Rodríguez, A. M.; Enriz, R. D.; Sosa, C. P.; Perczel, A.; Kucsman, A.; Farkas, O.; Deretey, E.; Vank, J. C.; Csizmadia, I. G. Can J Chem 2002, 80, 832.
7. Bombasaro, J. A.; Zamora, M. A.; Baldoni, H. A.; Enriz, R. D. J Phys Chem A 2005, 109, 874.
8. Klipfel, M. W.; Zamora, M. A.; Rodriguez, A. M.; Fidanza, N. G.; Enriz, R. D.; Csizmadia, I. G. J Phys Chem A 2003, 107, 5079.
9. Schäfer, L.; Siam, K.; Klimkowski, V. J.; Ewbank, J. D.; van Alsenoy, C. J Mol Struct (Theochem) 1990, 204, 361.
10. Schäfer, L.; Kulp-Newton, S. Q.; Siam, K.; Klimkowski, V. J.; van Alsenoy, C. J Mol Struct (Theochem) 1990, 209, 373.
11. Shirazian, S.; Gronert, S. J Mol Struct (Theochem) 1997, 397, 107.
12. Császár, A. G. J Am Chem Soc 1992, 114, 9569.
13. Császár, A. G. J Mol Struct 1995, 346, 141.
14. Császár, A. G. J Phys Chem 1996, 100, 3541.
15. Barroso, M. N.; Cerutti, E. S.; Rodriguez, A. M.; Jáuregui, E. A.; Farkas, O.; Perczel, A.; Enriz, R. D. J Mol Struct (Theochem) 2001, 548, 21.
16. Calaza, F. C.; Rigo, M. V.; Rinaldoni, A. N.; Masman, M. F.; Koo, J. C. P.; Rodríguez, A. M.; Enriz, R. D. J Mol Struct (Theochem) 2003, 634, 201.
17. Nir, E.; Janzen, C.; Imhof, P.; Kleinermans, K.; de Vrues, M. S. J Chem Phys 2001, 115, 4604.
18. Robertson, E. G.; Simons, J. P. Phys Chem Chem Phys 2001, 3, 1.
19. Zwier, T. S. J Phys Chem A 2001, 105, 8827.
20. Dian, B. C.; Longarte, A.; Winter, P. R.; Zwier, T. S. J Chem Phys 2004, 120, 133.
21. Bader, R. F. W. Atoms in Molecules. A Quantum Theory; Oxford University Press: Oxford, UK, 1990.
22. Foresman, J. B.; Keith, T. A.; Wiberg, K. B.; Snoonian, J. J Phys Chem 1996, 100, 16098.
23. IUPAC-IUB Commission on Biochemical Nomenclature. Biochemistry 1970, 9, 3471.
24. Ramachandran, I.; Sasisekharan, V. Adv Protein Chem 1968, 23, 283.
25. Frisch, M. J.; Trucks, G. W.; Schlegel, H. B.; Scuseria, G. E.; Robb, M. A.; Cheeseman, J. R.; Zakrzewski, V. G.; Montgomery, J. A., Jr.; Stratmann, R. E.; Burant, J. C.; Dapprich, S.; Millam, J. M.; Daniels, A. D.; Kudin, K. N.; Strain, M. C.; Farkas, O.; Tomasi, J.; Barone, V.; Cossi, M.; Cammi, R.; Mennucci, B.; Pomelli, C.; Adamo, C.; Clifford, S.; Ochterski, J.; Petersson, G. A.; Ayala, P. Y.; Cui, Q.; Morokuma, K.; Malick, D. K.; Rabuck, A. D.; Raghavachari, K.; Foresman, J. B.; Cioslowski, J.; Ortiz, V.; Baboul, A. G.; Stefanov, V.; Liu, G.; Liashenko, A.; Piskorz, P.; Komaromi, I.; Gomperts, R.; Martin, R. L.; Fox, D. J.; Keith, T.; Al-Laham, M. A.; Peng, C. Y.; Nanayakkara, A.; Gonzalez, C.; Challacombe, M.; Gill, P. M. W.; Johnson, B.; Chen, W.; Wong, M. W.; Andres, J. L.; Gonzalez, V.; Head-Gordon, M.; Replogle, E. S.; Pople, J. A. Gaussian 98; Revision A.7; Gaussian: Pittsburgh, PA, 1998.
26. Alemán, C.; Puiggalí, J. J Phys Chem B 1997, 101, 3441.
27. Improta, R.; Boarone, V.; Kudin, K. N.; Scuseria, G. E. J Chem Phys 2001, 114, 2541.
28. (a) Becke, A. D. Phys Rev A 1998, 38, 3098; (b) Becke, A. D. J Chem Phys 1993, 98, 5618; (c) Lee, C.; Yang, W.; Parr, R. G. Phys Rev B 1998, 37, 785.
29. Viviani, W.; Rivail, J.-L.; Perczel, A.; Csizmadia, I. G. J Am Chem Soc 1993, 115, 8321.
30. McAllister, M.; Endredi, G.; Viviani, W.; Perczel, A.; Császár, P.; Ladik, J.; Rivail, J.-L.; Csizmadia, I. G. Can J Chem 1995, 73, 563.
31. Popelier, P. L. A. Atoms in Molecules. An Introduction; Pearson Education: Harlow, UK, 1999.
32. Bader, R. F. W.; Essén, H. J Chem Phys 1984, 80, 1943.
33. Popelier, P. L. A.; Bader, R. F. W. Chem Phys Lett 1992, 189, 542.
34. Caroll, M. T.; Bader, R. F. W. Mol Phys 1988, 65, 695.
35. Koch, U.; Popelier, P. L. A. J Phys Chem 1995, 99, 9747.
36. Fidanza, N. G.; Suvire, F. D.; Sosa, G. L.; Lobayan, R. M.; Enriz, R. D.; Peruchena, N. M. J Mol Struct (Theochem) 2001, 543, 185.
37. Caroll, M. T.; Chang, C.; Bader, R. F. W. Mol Phys 1988, 63, 387.
38. Sosa, G. L.; Peruchena, N. M.; Contreras, R. H.; Castro, E. A. J Mol Struct (Theochem) 1997, 401, 77.
39. Sosa, G. L.; Peruchena, N. M.; Contreras, R. H.; Castro, E. A. J Mol Struct (Theochem) 2002, 577, 219.
40. (a) Coppens, P. X-Ray Charge Densities and Chemical Bonding; Oxford University Press: New York, 1997; (b) Wilson, K. S. Nat Struct Biol 1998, 5, 627.
41. Koritsánszky, T.; Flaig, R.; Zobel, D.; Krane, H. G.; Morgenroth, W.; Luger, P. Science 1998, 279, 356.
42. Klieger-Konig, W.; Bader, R. F. W.; Tan, T. H. J Comput Chem 1982, 3, 317.
43. Bader, R. F. W.; Johnson, S.; Tang, T. H.; Popelier, P. L. A. J Phys Chem 1996, 100, 15398.
44. Sieber, S.; Buzek, P.; Schleyer, P. V. R.; Kock, W.; Carneiro, J. W. M. J Am Chem Soc 1993, 115, 259.
45. Raghavachari, K.; Whiteside, R. A.; Pople, J. A.; Schleyer, P. V. R. J Am Chem Soc 1981, 103, 5649.
46. Carneiro, J. W. M.; Schleyer, P. v. R.; Saunders, M.; Remington, R.; Schaefer, H. F.; Rauk, A.; Sorensen, T. S. J Am Chem Soc 1994, 116, 3483.
47. Hiraoka, K.; Mori, T.; Yamabe, S. Chem Phys Lett 1993, 207, 178.
48. Miertus, S.; Scrocco, E.; Tomasi, J. Chem Phys 1981, 55, 117.
49. Iwaoka, M.; Okada, M.; Tomoda, S. J Mol Struct (Theochem) 2002, 586, 111.

50. Peterson, M. R.; Csizmadia, I. G. Prog Theor Org Chem 1982, 3, 190.
51. Csizmadia, I. G. New Theoretical Concept for Understanding Organic Reactions; Csizmadia, I. G.; Bertran, J. D., Eds.; Reidel: Dordrecht, Netherlands, 1989.
52. Gould, R. O.; Gray, A. M.; Taylor, P.; Walkinshaw, M. D. J Am Chem Soc 1985, 107, 5921.
53. Canossa Koolman, H.; Rousseau, R. W. AIChE J 1996, 42, 147.
54. Givand, J. C.; Rousseau, R. W.; Ludovice, P. J. J Crystal Growth 1998, 194, 228.
55. Havlin, R. H.; Le, H.; Laws, D. D.; de Dios, A. C.; Oldfield, E. J Am Chem Soc 1997, 119, 11951.
56. Perczel, A.; Angyán, J. G.; Kajtár, M.; Viviani, W.; Rivail, J.-L.; Marcoccia, J.-F.; Csizmadia, I. G. J Am Chem Soc 1991, 113, 6256.
57. McAllister, M. A.; Perczel, A.; Csaszar, P.; Viviani, W.; Rivail, J.-L.; Csizmadia, I. G. J Mol Struct (Theochem) 1993, 288, 161.
58. Bombasaro, J. A.; Rodríguez, A. M.; Enriz, R. D. J Mol Struct (Theochem) 2005, 724, 173.
59. Born, M. Z Phys 1920, 1, 45.
60. Onsager, L. J Am Chem Soc 1936, 58, 1486.
61. Kirkwood, J. G. J Chem Phys 1934, 2, 351.
62. Shang, H. S.; Head-Gordon, T. J Am Chem Soc 1994, 116, 1528.
63. Head-Gordon, T.; Head-Gordon, M.; Frisch, M. J.; Brooks, C. L., III; Pople, J. A. J Am Chem Soc 1991, 113, 5989.
64. Alemán, C. J Phys Chem A 2000, 104, 7612.